CONFIDENTIAL

N 62 62893 175

Copy
RM E54H25

NACA RM E54H25

NACA

RESEARCH MEMORANDUM

EFFECT OF DIVERGENCE ANGLE ON THE INTERNAL PERFORMANCE CHARACTERISTICS OF SEVERAL CONICAL CONVERGENT-DIVERGENT NOZZLES

By Fred W. Steffen, H. George Krull, and Ralph F. Schmiedlin

Lewis Flight Propulsion Laboratory
Cleveland, Ohio

CLASSIFICATION CHANGED TO UNCLASSIFIED
AUTHORITY: PUBLICATION ANNOUNCEMENT NO. 1
EFFECTIVE DATE: SEPTEMBER 17, 1958

CLASSIFIED DOCUMENT

This material contains information affecting the National Defense of the United States within the meaning of the espionage laws, Title 18, U.S.C., Secs. 793 and 794, the transmission or revelation of which in any manner to an unauthorized person is prohibited by law.

NATIONAL ADVISORY COMMITTEE
FOR AERONAUTICS

WASHINGTON
November 29, 1954

CONFIDENTIAL

NATIONAL ADVISORY COMMITTEE FOR AERONAUTICS

RESEARCH MEMORANDUM

EFFECT OF DIVERGENCE ANGLE ON THE INTERNAL PERFORMANCE CHARACTERISTICS OF SEVERAL CONICAL CONVERGENT-DIVERGENT NOZZLES

By Fred W. Steffen, H. George Krull, and Ralph F. Schmiedlin

3491

CW-1

SUMMARY

Experiments were conducted on conical convergent-divergent nozzles having included divergence angles from 7° 10' to 50° and expansion ratios from 1.39 to 3.81 over a wide range of nozzle pressure ratios with cold flow, to determine the effect of divergence angle on the internal performance of the nozzles.

Thrust coefficients at design pressure ratios decreased from 0.973 at a divergence angle of 7° 10' to 0.930 at a divergence angle of 50°. Similar trends were noted at pressure ratios slightly less than and greater than design.

At pressure ratios where separation occurred within the nozzle, improved performance was effected by increasing the divergence angle.

At any given divergence angle, a change in expansion ratio had negligible effect on nozzle performance at design pressure ratio.

Although divergence angle and expansion ratio were found to have no effect on nozzle flow coefficient at choked pressure ratios, the pressure ratio required to choke the nozzle increased with an increase in divergence angle.

INTRODUCTION

The selection of a convergent-divergent exhaust nozzle for operation at high nozzle pressure ratios requires consideration of both the expansion ratio and divergence angle. For a particular expansion ratio, a short high-divergence nozzle would have low weight and low cooling-

surface area. As shown in reference 1, such nozzles would also promote flow separation at low nozzle pressure ratios, thus relieving overexpansion losses. On the other hand, reference 1 also indicates that better performance at pressure ratios close to the isentropic design value is provided by long, low-divergence nozzles.

Some data on the effect of divergence angle on nozzle performance are presented in reference 2, but the range of divergence angles covered was extremely small (0° to 7° 10') and no significant effects were observed. The data of reference 1 also do not permit the effects of divergence angle to be isolated because each divergence angle was associated with a different expansion ratio.

3491

The purposes of the investigation reported herein are to determine the isolated effect of divergence angle on nozzle internal performance and the variation of nozzle internal performance over a wide range of divergence angles. Data for nozzles of approximately equal throat size which vary in divergence angle from 7° 10' to 50° and in expansion ratio from 1.39 to 3.81 are included in the report. All nozzles were run with cold flow over a range of nozzle pressure ratios from well below design to about design or greater.

APPARATUS AND INSTRUMENTATION

Nozzles

Nozzles of six different divergence angles, namely 7° 10', 11° 50', 24°, 30°, 36°, and 50° were investigated. Details of the nozzles are shown in figure 1, and in the following table:

Nozzle divergence angles	Nozzle expansion ratios				
7° 10'	1.39	1.69	---	2.65	----
11° 50'	1.39	1.69	---	2.65	----
24°	1.39	1.69	---	2.65	----
30°	----	----	1.8	----	----
36°	----	----	1.8	----	----
50°	----	1.69	---	2.65	3.81

The nozzles having divergence angles of 7° 10', 11° 50', and 24° were run at expansion ratios of 1.39, 1.69 and 2.65. The 30° and 36° nozzles were run at an expansion ratio of 1.8 only, whereas the 50° nozzle was run at expansion ratios of 1.69, 2.65, and 3.81.

All nozzles had 13-inch-diameter inlets, 50° conical convergent sections, 7-inch-radius circular-arc throat contours, and conical divergent sections. With the exception of the 30° nozzle which had a 7.16-inch-diameter throat, all nozzles had approximately 6-inch-diameter throats.

3491 CW-1 back

Installation

The installation of the nozzles in the test rig is shown in figure 2. The nozzles were fastened to the mounting pipe which was in turn attached to a bed plate freely suspended from four flexure rods. The entire assembly was installed within a plenum chamber connected on one end to the laboratory high-pressure air supply and on the other end to the laboratory altitude exhaust system. Pressure difference across the nozzle and mounting pipe was maintained by labyrinth seals around the mounting pipe. A vent line between the two labyrinth seals and the plenum chamber decreased the pressure differential across the second labyrinth seal and prevented dynamic pressures from acting on the outside of the diffuser section. Forces acting on the nozzle and mounting pipe, both external and internal, were transmitted from the bed plate through a flexure-plate supported bell crank and linkage to a balanced air-pressure diaphragm force-measuring cell.

Instrumentation

Pressures and temperatures were measured at various stations as shown in figure 2. Pressures obtained from total-pressure rakes and wall static taps at stations 1 and 2 were used in the computation of inlet momentum and air flow, respectively. Total-pressure and total-temperature rakes were installed at station n to determine nozzle-inlet conditions. Plenum chamber static pressure and the static pressure acting on the outside of the bellmouth inlet were obtained from taps located along the outer surfaces of the nozzle and the nozzle mounting pipe. Inside wall static taps from nozzle throat to nozzle exit were used to measure pressure distributions in the divergent sections of the nozzles.

PROCEDURE

Performance data for all nozzles were obtained over a range of pressure ratios from well below design to about design or greater.

Pressure-ratio variation was obtained by variation of exhaust pressure while inlet pressure and weight flow were held approximately constant; inlet pressures were about 35 and 25 pounds per square inch absolute for the 6- and 7.16-inch-throat-diameter nozzles, respectively.

Unheated dry air at a temperature of about 80° F, shown in reference 1 to be sufficient to eliminate condensation shock, was used for the entire investigation. Symbols and methods of calculation are given in appendixes A and B, respectively.

3491

RESULTS AND DISCUSSION

Typical Performance Characteristics

Thrust performance of all the nozzles investigated as a function of nozzle pressure ratio is shown in figure 3. Data for nozzles having equal expansion ratios but different divergence angles are presented in each part of the figure. For all nozzles other than the 50° nozzle, peak thrust coefficient occurs at the design pressure ratio, which is defined as the one-dimensional isentropic pressure ratio corresponding to the given expansion ratio. The peak thrust coefficients of the 50° nozzles appear in the range of nozzle pressure ratios from 2 to 3.

Effects of Divergence Angle on Thrust Coefficient at Pressure Ratios Close to Design and Above

From figure 3, parts (b) and (d) particularly, it can be seen that the thrust coefficient, at pressure ratios close to the design value and above, decreases with an increase in divergence angle. This effect is clearly indicated in figure 4, a cross plot of figure 3, which presents thrust coefficient at design pressure ratio against divergence angle. At design pressure ratio, the thrust coefficient decreased from about 0.973 at a divergence angle of 7° 10' to 0.930 at a divergence angle of 50°. Data for pressure ratios slightly less than or greater than design pressure ratio would show a similar trend.

A theoretical curve noting the variation of thrust coefficient with divergence angle is also included in figure 4. The equation $C_T = \frac{1}{2}\left(1 + \cos\frac{\alpha}{2}\right) C_{T(\alpha=0)}$ was used to calculate the points on the curve. If any radial variation of velocity or density at the nozzle exit is neglected, the term $\frac{1}{2}\left(1 + \cos\frac{\alpha}{2}\right)$ is approximately equal to the ratio of the axial component of the discharge momentum to the total discharge

momentum. In order to adjust the level of the theoretical curve to the level of the experimental data, it was assumed that a nozzle having a completely axial discharge would have a thrust coefficient of 0.975. The agreement between the experimental data and the theoretical curve is good.

At a given divergence angle, the variation in thrust coefficient with expansion ratio at design pressure ratio was small, even though changes in wetted area of the divergent section were large. For example, changing the expansion ratio of the 7° 10' nozzle from 1.39 to 2.65 resulted in a 317 percent increase in the wetted area of the divergent section without effecting any significant change in thrust coefficient.

3491

Some indication of the variation in thrust performance with divergence angle at pressure ratios around and above design can be determined from the internal wall pressure distributions in the divergent sections of the nozzles. These pressure distributions are shown in figure 5. Deviations of the wall pressures from the one-dimensional isentropic-pressure distribution are caused by three-dimensional expansions and compressions. The area under these curves is indicative of the amount of thrust provided by the divergent sections of the nozzles, the greater the area the greater the thrust. Values of thrust coefficients calculated from pressure distributions in the divergent sections of the nozzles are shown in figure 6. For the calculations, it was assumed that all the nozzles represented in figure 5 were operated at an expansion ratio of 1.8 and at a nozzle pressure ratio of 8.9, the design pressure ratio corresponding to the expansion ratio. A curve of thrust coefficient obtained from force measurements is also shown in figure 6. Thrust coefficients calculated from pressures show a decrease with an increase in divergence angle similar to that obtained from force measurements.

Effect of Divergence Angle on Overexpanded Performance

From the data in figure 3, particularly parts (c) and (d), it can be seen that at low nozzle pressure ratios, where separation occurs, nozzle thrust performance is improved by an increase in divergence angle. This effect is shown in figure 7, a cross plot of data from nozzles of various design pressure ratios (expansion ratios), all operating at a nozzle pressure ratio of 2. Increasing the divergence angle improves nozzle performance by influencing the overexpanded flow to experience a shock and to separate from the nozzle walls at locations progressively closer to the throat, thus decreasing the area acted upon by lower-than-ambient pressures. Movement of the shock, and thus separation point, towards the throat of the nozzle with increasing divergence angle is indicated in figure 8 by a typical pressure distribution curve. Data are presented for nozzles having various divergence angles and an expansion ratio of 2.65 operating at a pressure ratio of 4.

After the flow separated from the nozzle walls, it was observed to become essentially axial. Thus, for the 50° nozzle, which peaks at nozzle pressure ratios from about 2 to 3, the separated axial flow provided a greater part of the ideally available momentum in the axial direction than did the attached nonaxial flow at design pressure ratio.

Effect of Divergence Angle on Nozzle Air-Flow Characteristics

Weight-flow parameter (corrected weight flow per unit throat area, lb/(sec)(sq in.)) at pressure ratios where the flow was choked was unaffected by either nozzle divergence angle or expansion ratio, as shown in figure 9. A high divergence angle does, however, cause the nozzle to choke at higher pressure ratios. Nozzles having divergence angles of 24° or greater generally choked at a pressure ratio of 1.8, while the others were already choked at a pressure ratio of 1.2.

The values of the flow coefficients at choked conditions (the ratios of the measured values of the flow parameter to its theoretical value, 0.344 lb/(sec)(sq in.)) were very high; a mean value of the data indicates flow coefficients close to 1.000.

SUMMARY OF RESULTS

Conical convergent-divergent nozzles having divergence angles from 7° 10' to 50° and expansion ratios from 1.39 to 3.81 were run over a wide range of nozzle pressure ratios to determine the variation of nozzle internal performance with divergence angle.

At design pressure ratio, the thrust coefficient decreased from 0.973 at a divergence angle of 7° 10' to 0.930 at a divergence angle of 50°. At pressure ratios above design and slightly less than design, nozzle thrust coefficient also decreased with an increase in divergence angle.

For a nozzle having a given expansion ratio and pressure ratio, and operating with separated flow, the separation point occurred closer to the throat for the high angle nozzles, thus relieving overexpansion losses. Therefore, at pressure ratios considerably below design, nozzle performance improved with an increase in divergence angle.

At a given divergence angle, thrust coefficient at design pressure ratio was relatively unaffected by changes in expansion ratio within the range of expansion ratios and divergence angles investigated.

Peak thrust coefficients for all nozzles except those having a 50° divergence angle occurred at the design pressure corresponding to the

3491

given expansion ratio. The 50° nozzles, however, peaked at nozzle pressure ratios between about 2 and 3 apparently because of almost complete separation at these pressure ratios.

Flow coefficients at pressure ratios sufficient to choke the nozzles were unaffected by either divergence angle or expansion ratio, and appeared to be very close to 1.000. The pressure ratio required to choke the nozzles increased with an increase in divergence angle.

3491

Lewis Flight Propulsion Laboratory
National Advisory Committee for Aeronautics
Cleveland, Ohio, September 10, 1954

APPENDIX A

SYMBOLS

The following symbols are used in this report:

A	area, sq ft, (sq in. in fig. 9)
A_l	effective pipe area under labyrinth seals, sq ft
C_T	thrust coefficient
F	thrust, lb
F_d	resultant force on thrust cell (balanced-air-pressure-diaphragm force), lb
g	acceleration due to gravity, 32.174 ft/sec^2
P	total pressure, lb/sq ft
p	static pressure, lb/sq ft
R	gas constant, 53.3 ft lb/(lb)($^\circ$R)
T	total temperature, $^\circ$R
V	velocity, ft/sec
W_a	measured air flow, lb/sec
α	nozzle divergence angle
γ	ratio of specific heats, 1.4
δ	ratio of total pressure at nozzle inlet to absolute pressure at NACA standard sea-level conditions
θ	ratio of total temperature at nozzle inlet to absolute temperature at NACA standard sea-level conditions

Subscripts:

bm	outside of bellmouth inlet
e	nozzle exit

3491

i	ideal
j	jet
n	nozzle inlet
t	nozzle throat
w	wall
x	axial
0	exhaust or ambient
1	mounting pipe inlet station
2	air-flow measuring station

3491 CM-2

APPENDIX B

Air flow. - The nozzle air flow was calculated as

$$W_a = \frac{A_2 p_{2,w}}{\sqrt{RT_n}} \sqrt{\frac{2g\gamma}{\gamma-1}\left[\left(\frac{P_2}{p_{2,w}}\right)^{\frac{\gamma-1}{\gamma}} - 1\right]\left(\frac{P_2}{p_{2,w}}\right)^{\frac{\gamma-1}{\gamma}}}$$

with γ assumed to be 1.4.

Thrust. - The jet thrust was defined as

$$F_j = \frac{W_a V_{e,x}}{g} + A_e(p_e - p_0)$$

and was calculated by the equation

$$F_j = p_{1,w}A_1 + \frac{W_a V_1}{g} - p_{bm}A_1 + A_7(p_{bm} - p_0) - F_d$$

where F_d was obtained from balanced-air-pressure-diaphragm measurements. The ideally available jet thrust, which was based on measured mass flow, was calculated as

$$F_i = W_a \sqrt{\frac{2R}{g}\frac{\gamma}{\gamma-1} T_n \left[1 - \left(\frac{p_0}{P_n}\right)^{\frac{\gamma-1}{\gamma}}\right]}$$

Thrust coefficient. - The thrust coefficient is defined as the ratio of the actual to the ideal jet thrust:

$$C_T = \frac{F_j}{F_i}$$

3491

REFERENCES

1. Krull, H. George, and Steffen, Fred W.: Performance Characteristics of One Convergent and Three Convergent-Divergent Nozzles. NACA RM E52H12, 1952.

2. Fradenburgh, Evan A., Gorton, Gerald C., and Beke, Andrew: Thrust Characteristics of a Series of Convergent-Divergent Exhaust Nozzles At Subsonic and Supersonic Flight Speeds. NACA RM E53L23, 1954.

3491

CW-2 back

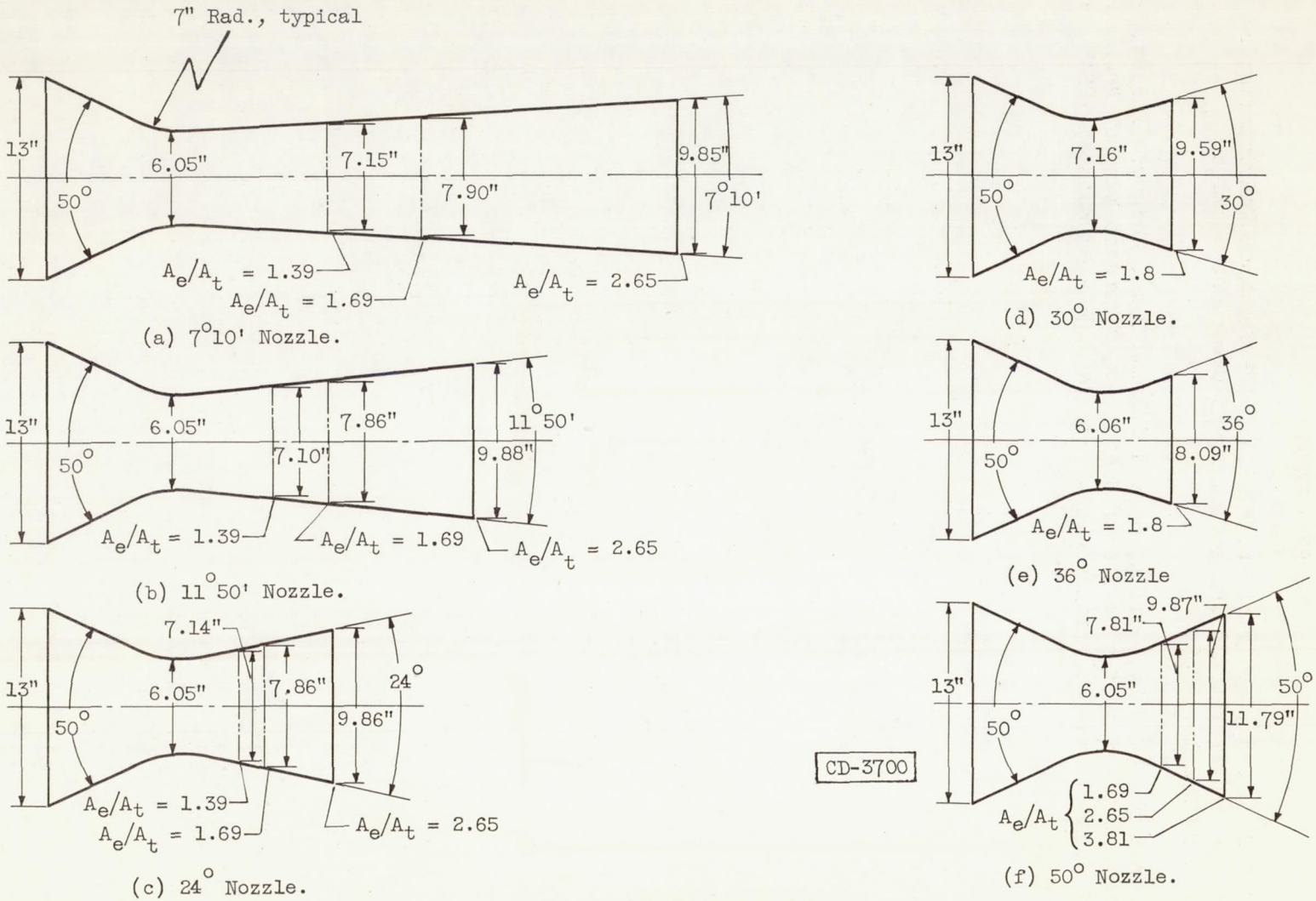


Figure 1. - Schematic diagrams of convergent-divergent nozzles.

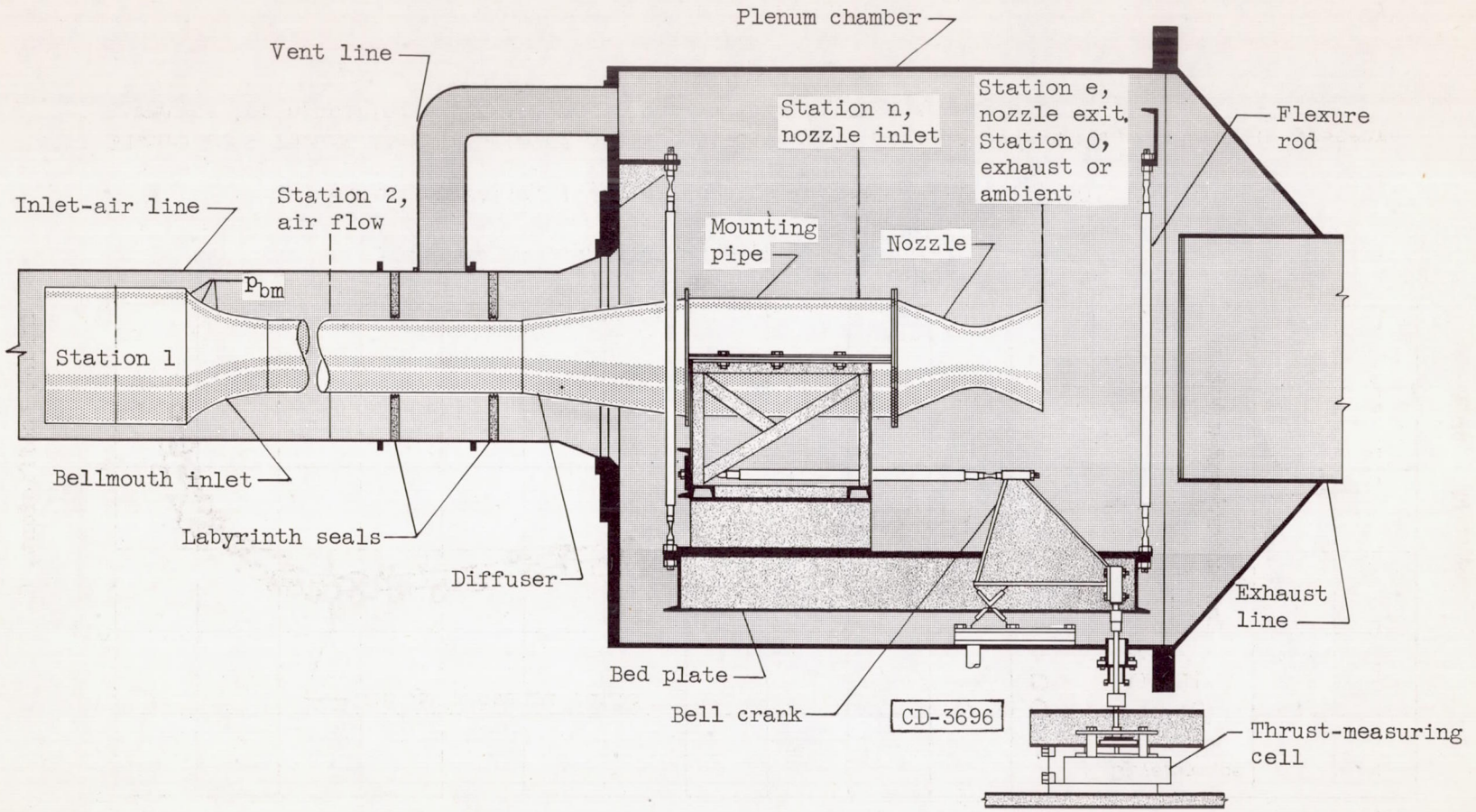
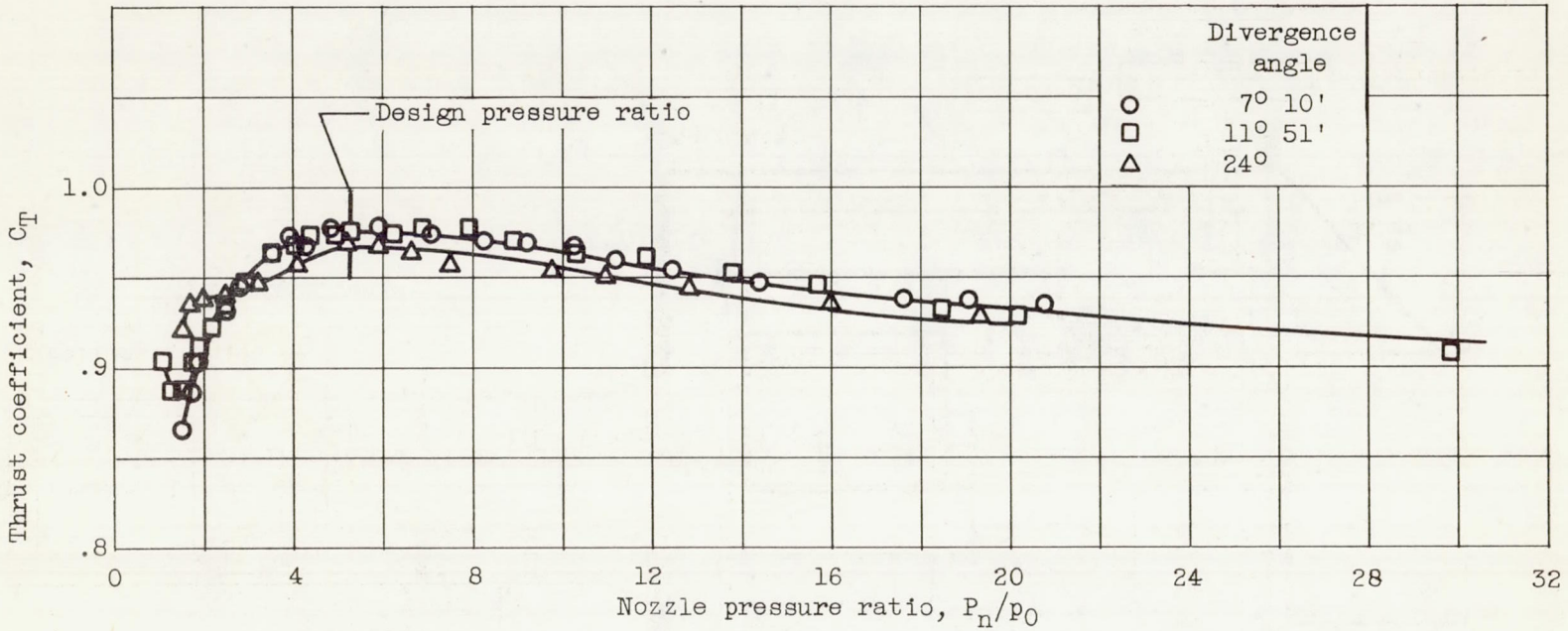


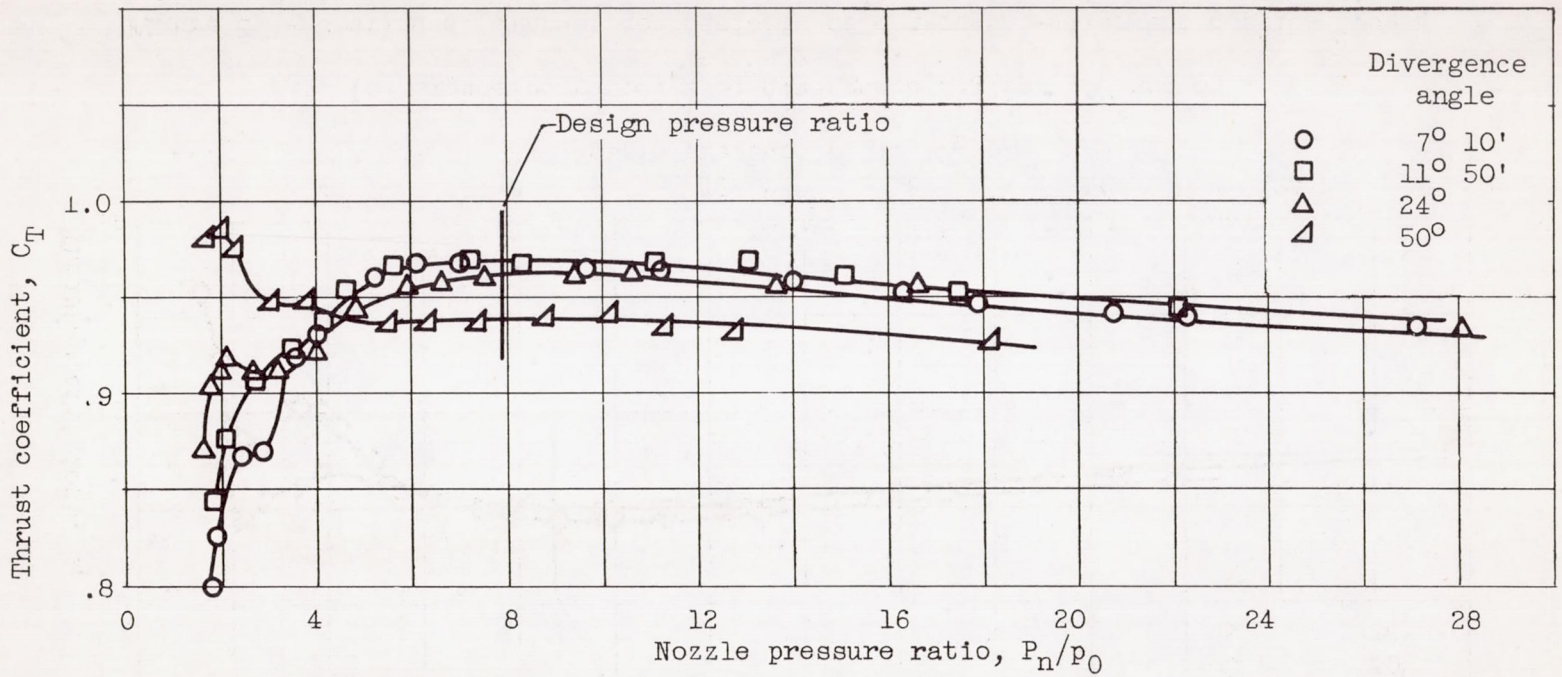
Figure 2. - Installation of nozzle in test chamber.

CONFIDENTIAL



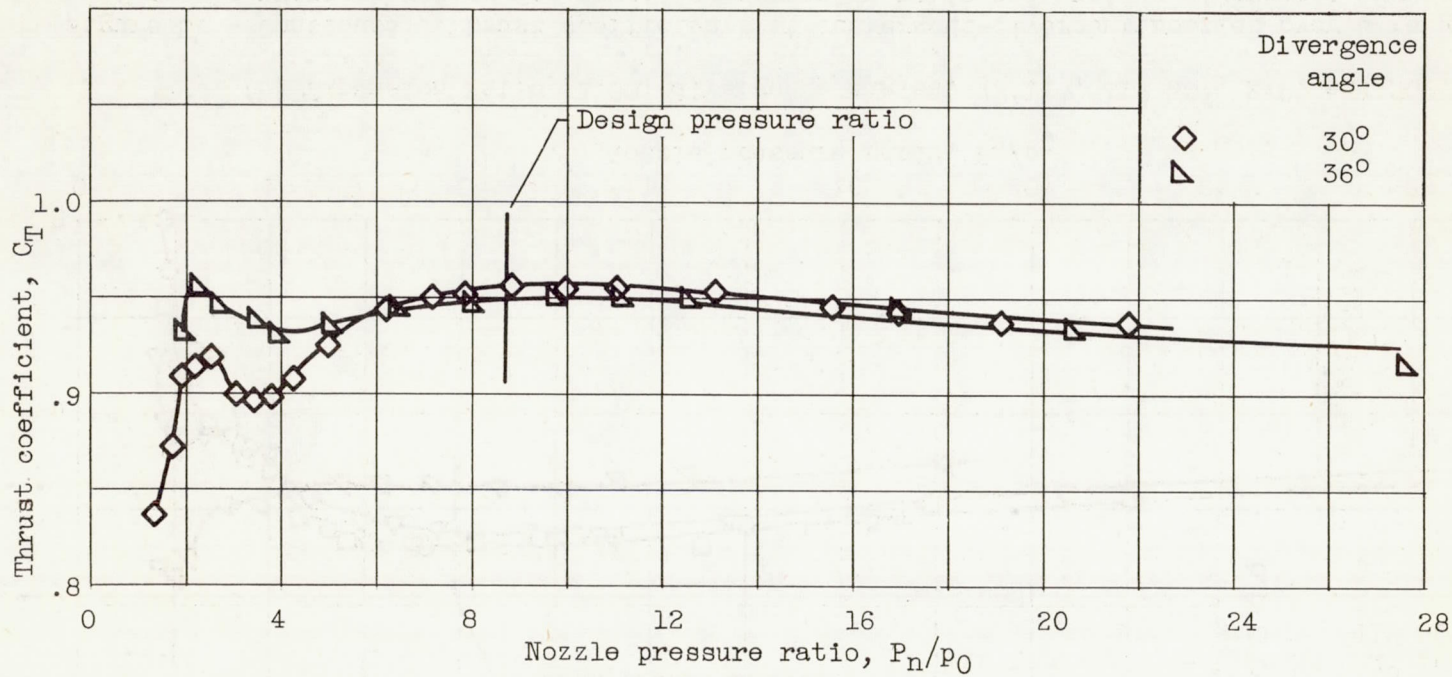
(a) Expansion ratio, 1.39; divergence angles, 7° 11', 11° 50', and 24°.

Figure 3. - Thrust coefficients of convergent-divergent nozzles over a range of nozzle pressure ratios for specified expansion ratio and various divergence angles.



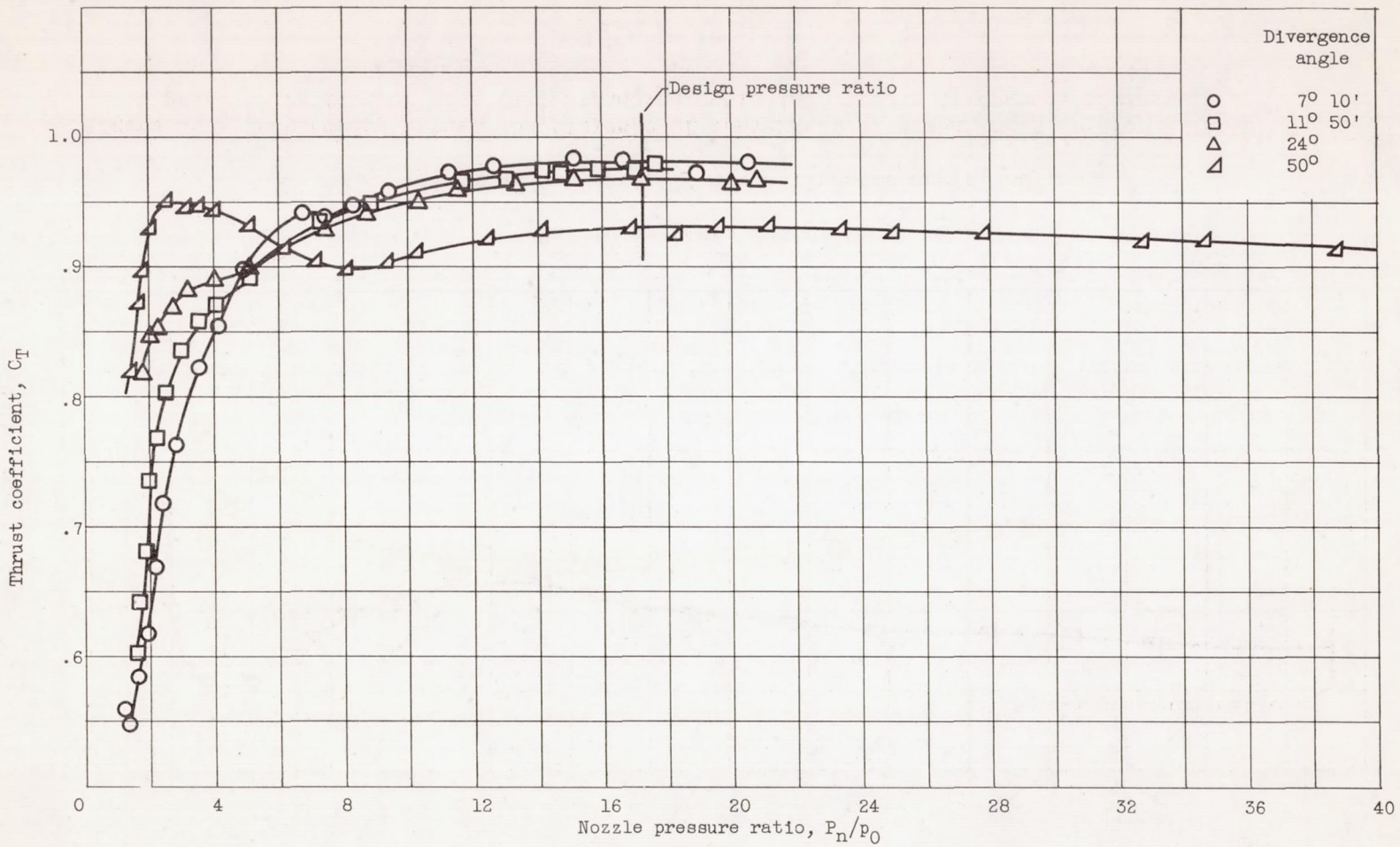
(b) Expansion ratio, 1.69; divergence angles, 7° 11', 11° 50', 24°, and 50°.

Figure 3. - Continued. Thrust coefficients of convergent-divergent nozzles over a range of nozzle pressure ratios for specified expansion ratio and various divergence angles.



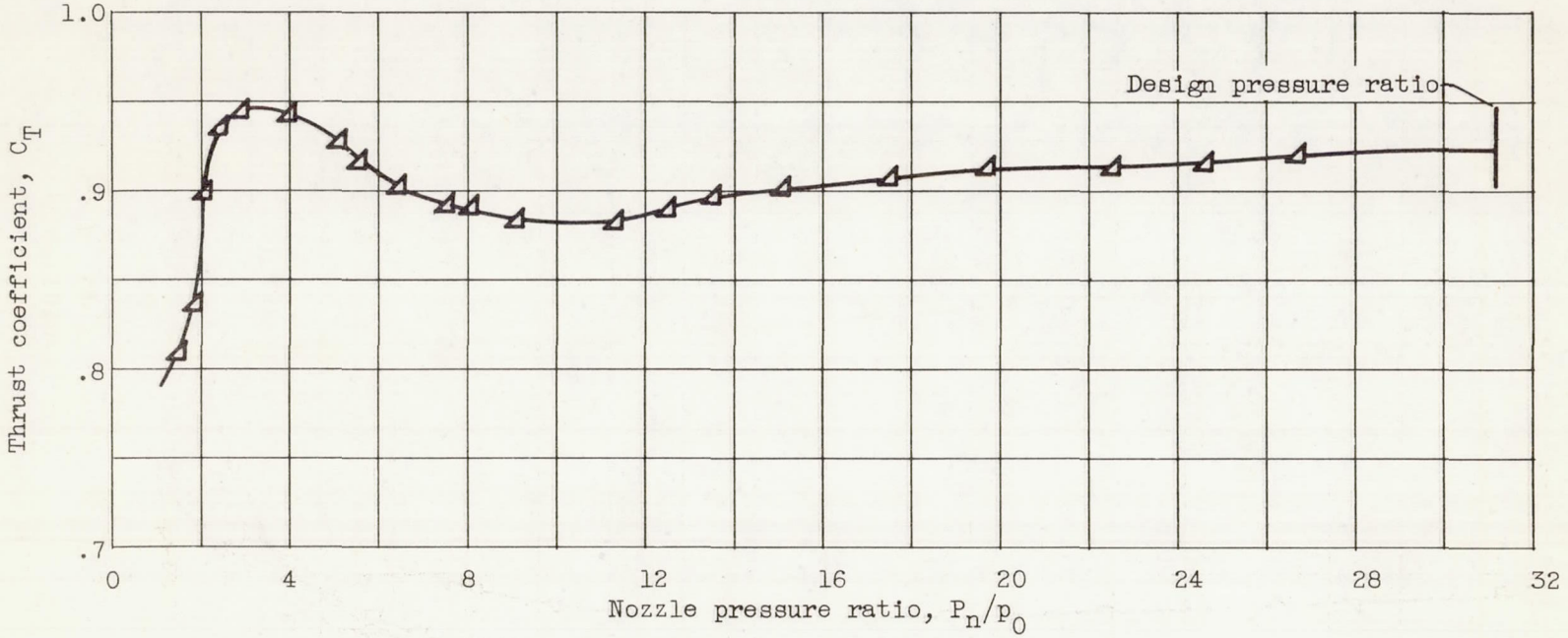
(c) Expansion ratio, 1.8; divergence angles, 30° and 36°.

Figure 3. - Continued. Thrust coefficients of convergent-divergent nozzles over a range of nozzle pressure ratios for specified expansion ratio and various divergence angles.



(d) Expansion ratio, 2.65; divergence angles, 7° 10', 11° 50', 24°, and 50°.

Figure 3. - Continued. Thrust coefficients of convergent-divergent nozzles over a range of nozzle pressure ratios for specified expansion ratio and various divergence angles.



(e) Expansion ratio, 3.81; divergence angle, 50°.

Figure 3. - Concluded. Thrust coefficients of convergent-divergent nozzles over a range of nozzle pressure ratios for specified expansion ratio and various divergence angles.

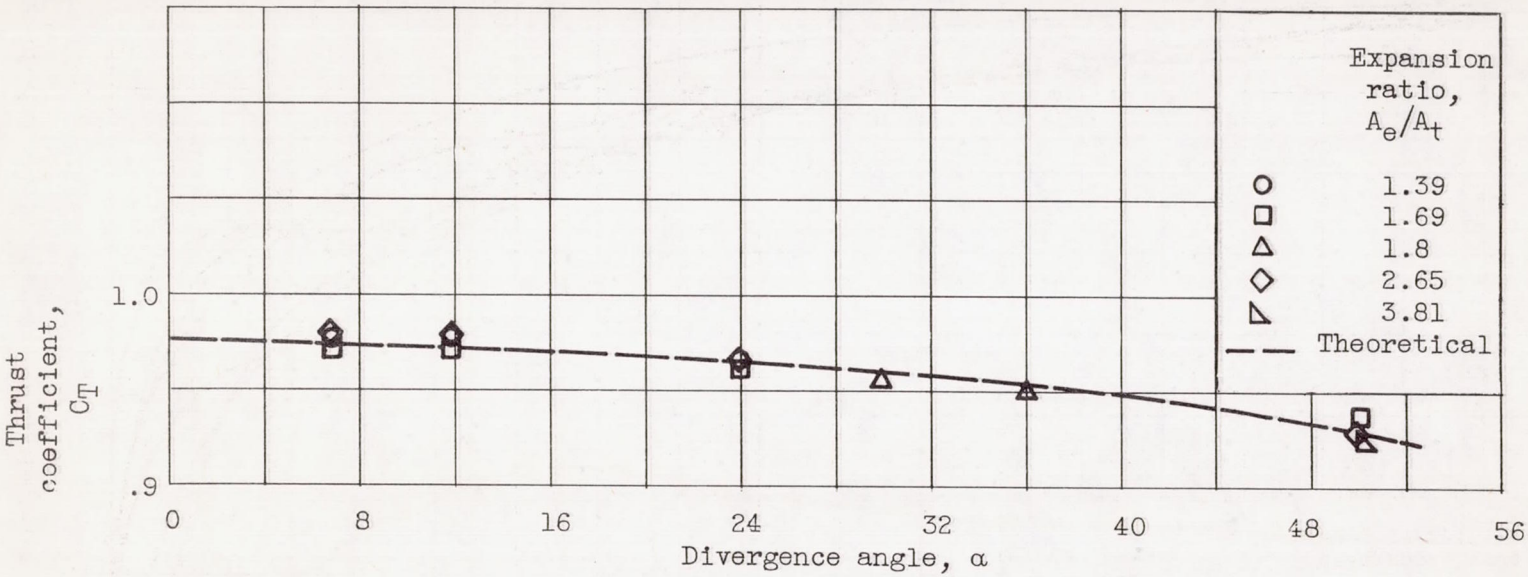


Figure 4. - Variation in thrust coefficient at design nozzle pressure ratio with nozzle divergence angle.

CONFIDENTIAL

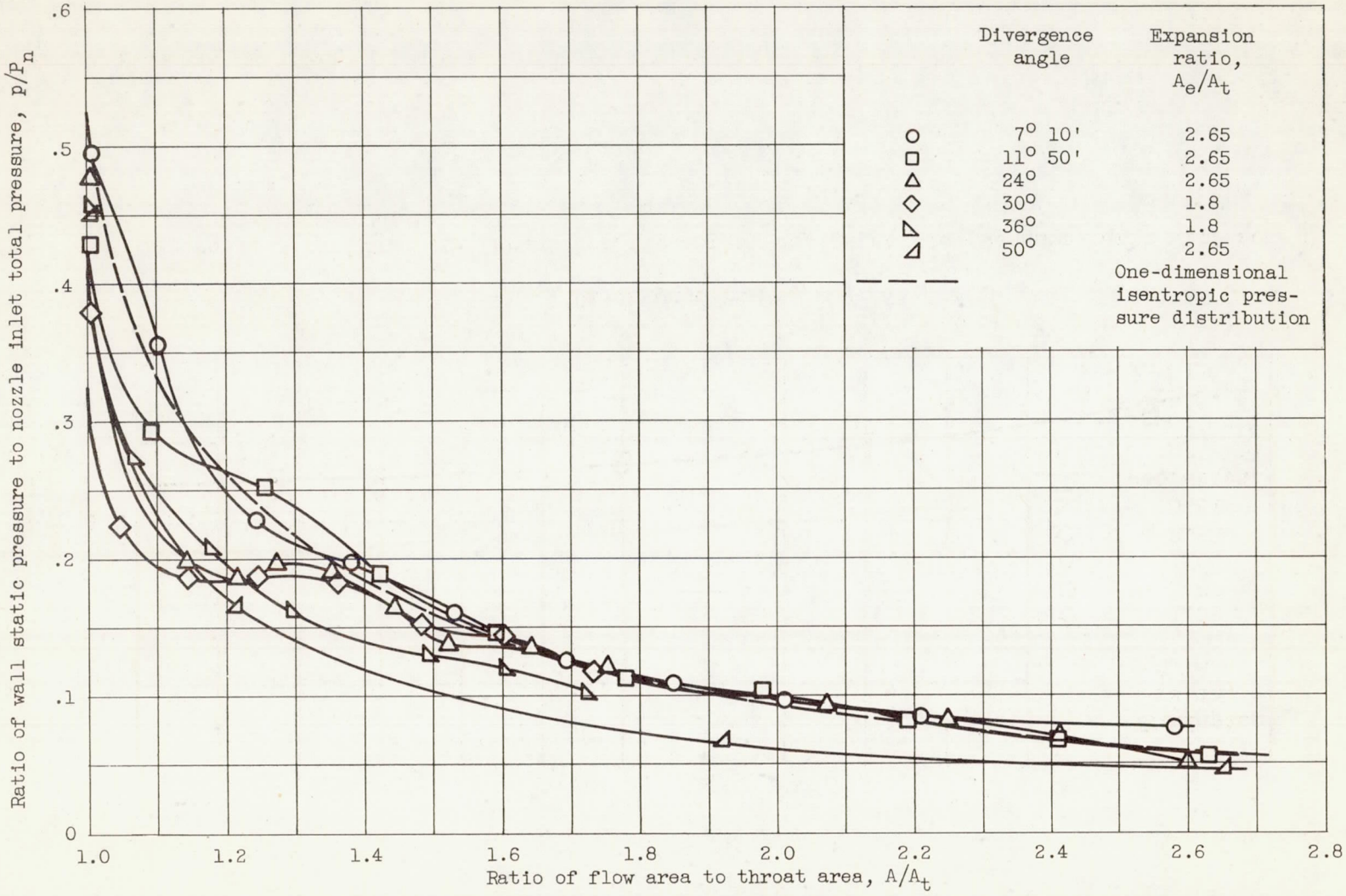


Figure 5. - Generalized pressure distributions along divergent walls of several convergent-divergent nozzles having various divergence angles at nozzle pressure ratios at or above design.

CONFIDENTIAL

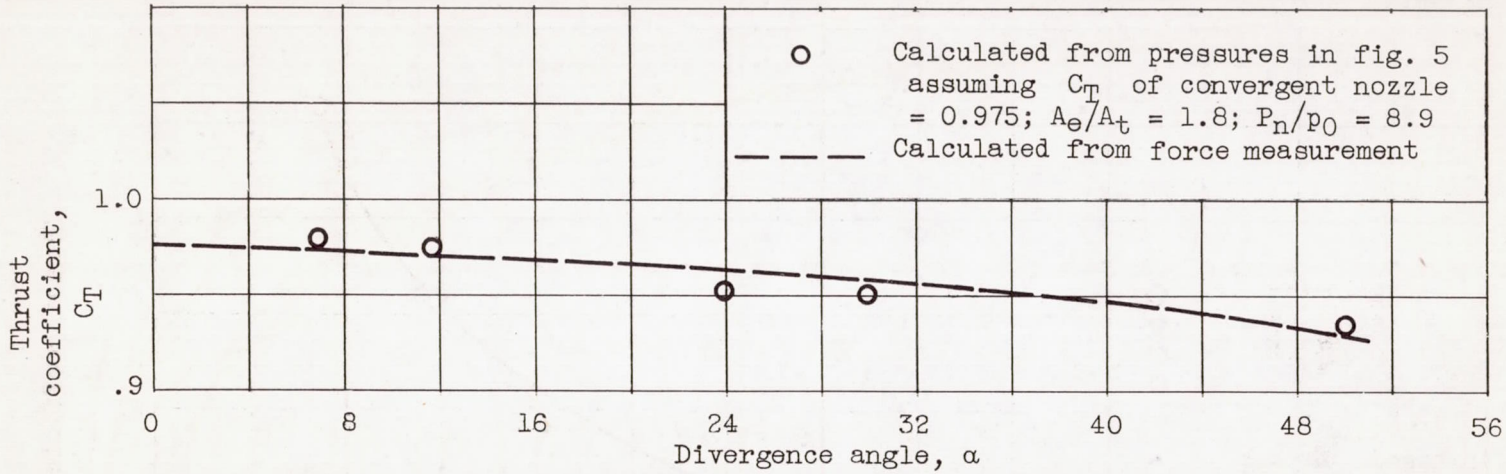


Figure 6. - Variation in thrust coefficient calculated from pressure distributions in divergent sections of nozzles at design pressure ratio with nozzle divergence angle.

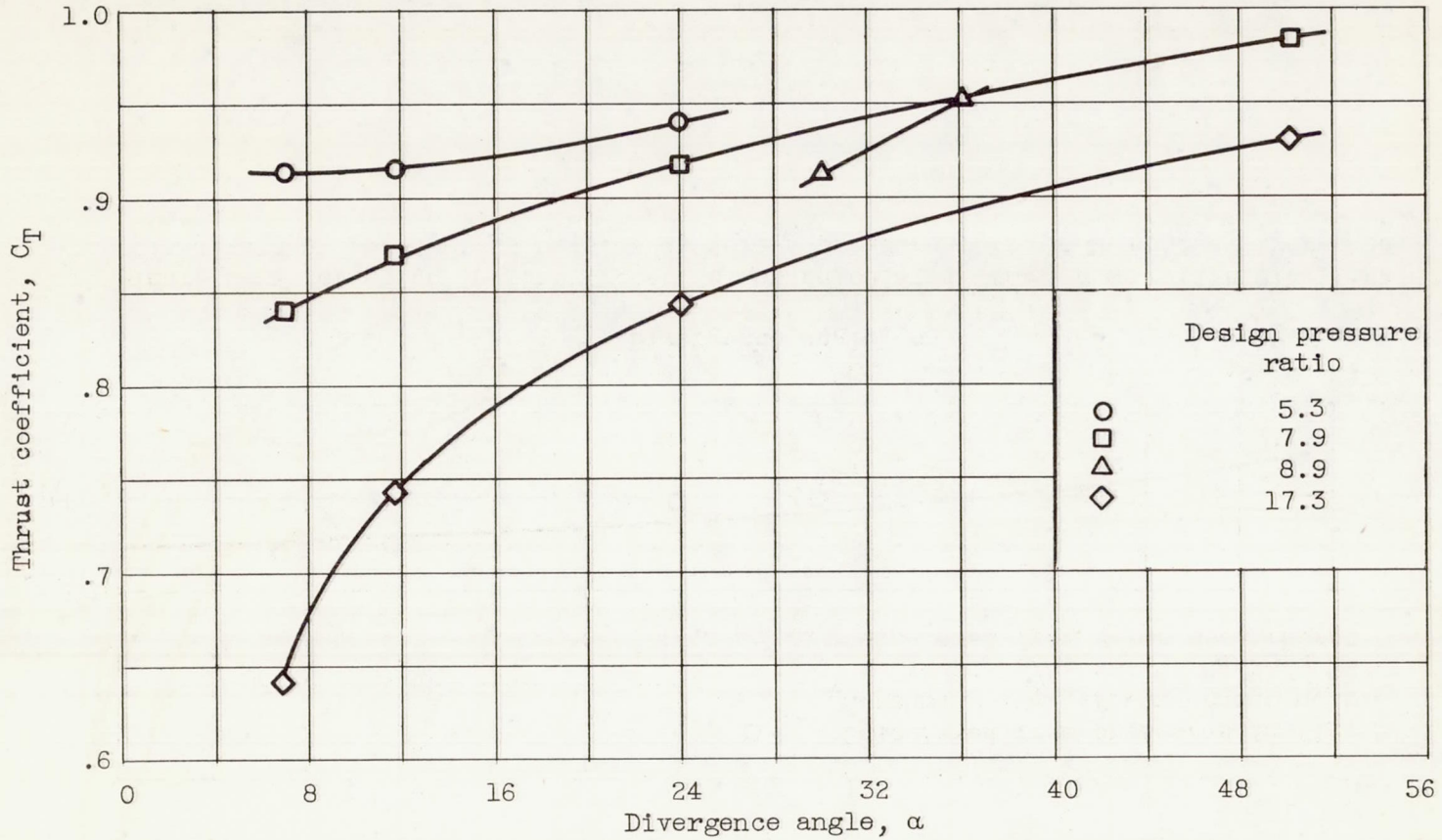


Figure 7. - Variation in thrust coefficient at a nozzle pressure ratio of 2.0 with divergence angle for nozzles of various design pressure ratios.

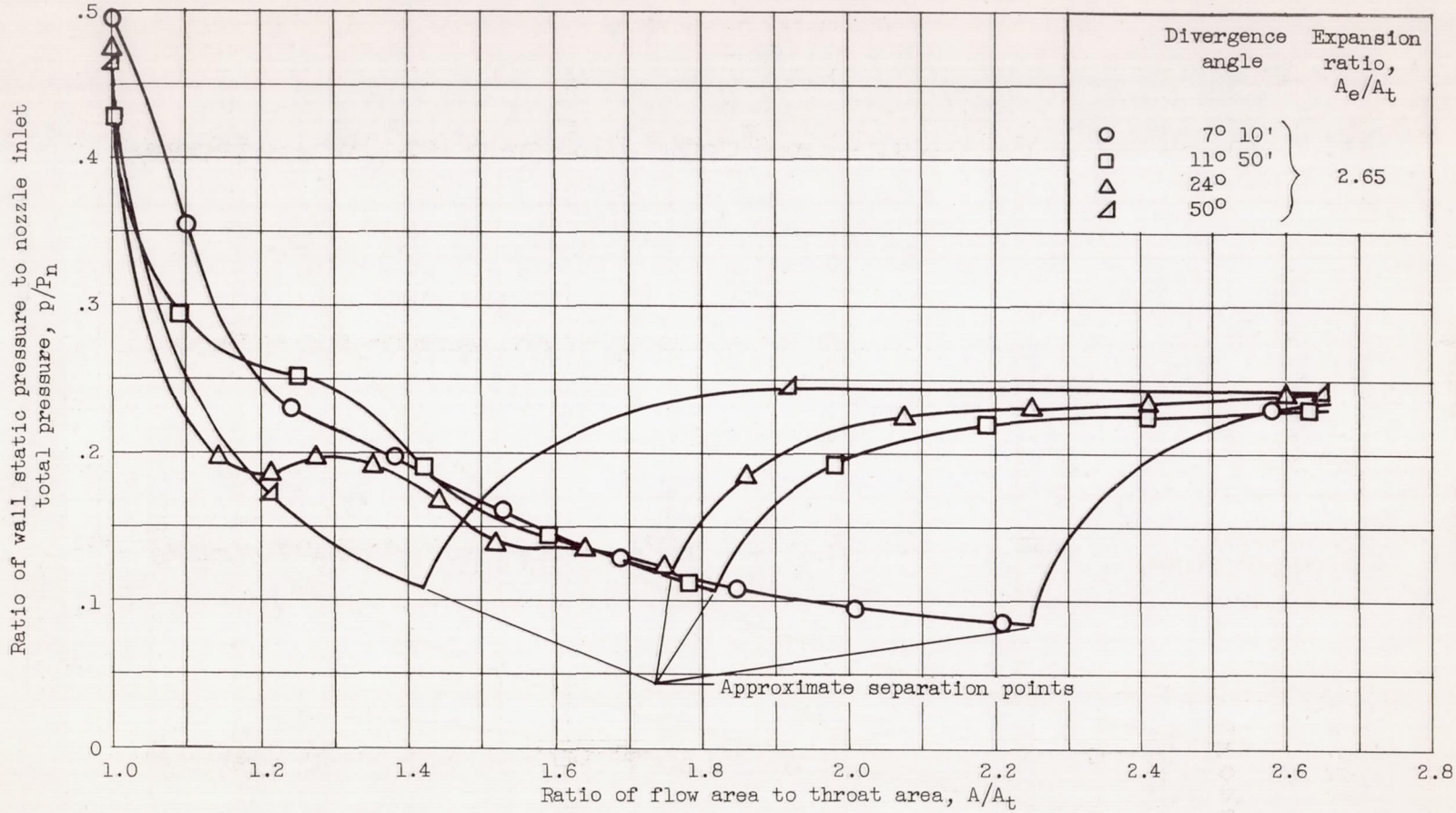
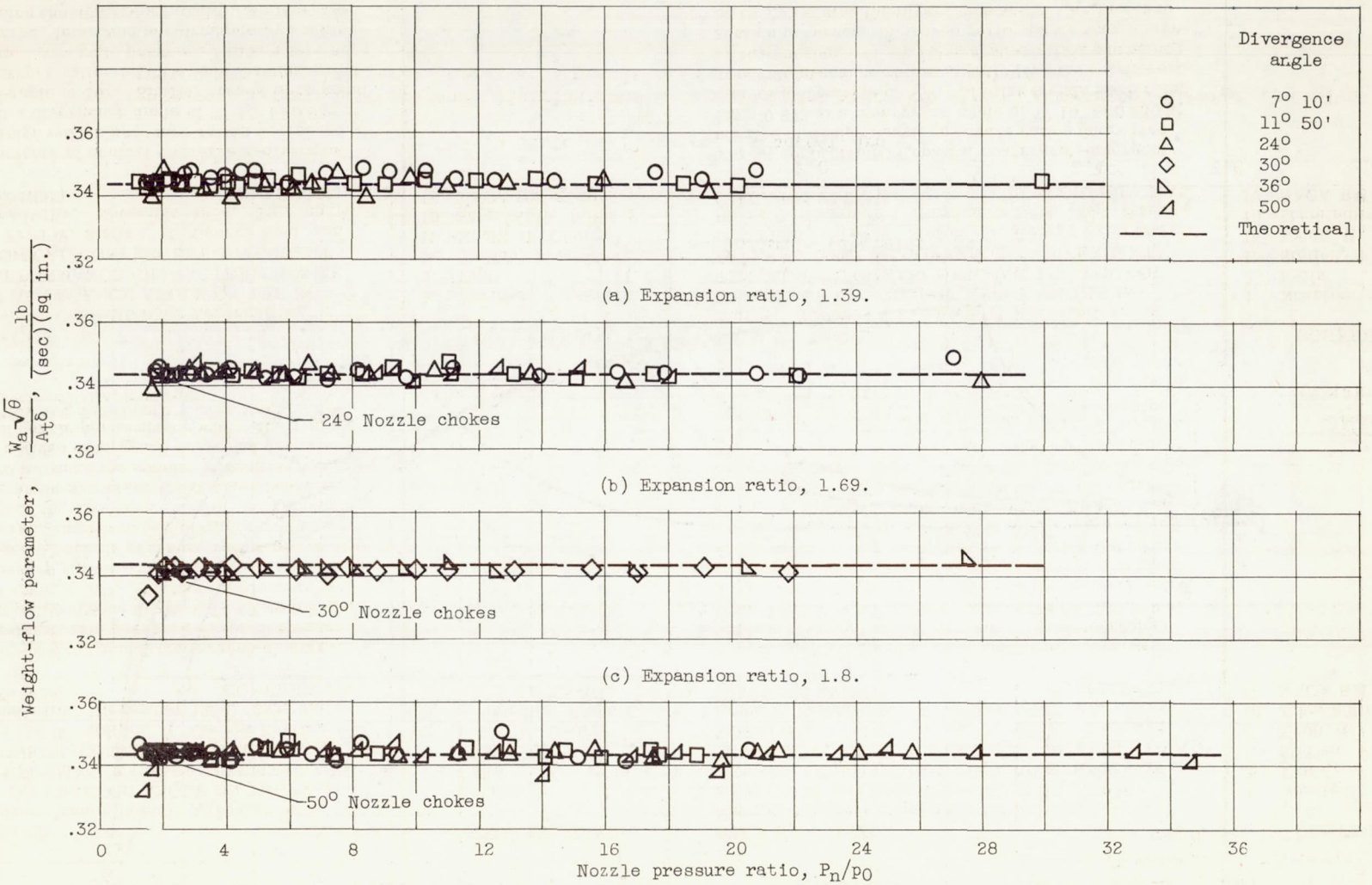


Figure 8. - Generalized pressure distributions along divergent walls of several convergent-divergent nozzles having various divergence angles at a nozzle pressure ratio of approximately 4.



(a) Expansion ratio, 1.39.

(b) Expansion ratio, 1.69.

(c) Expansion ratio, 1.8.

(d) Expansion ratio, 2.65.

Figure 9. - Variation in weight-flow parameter with nozzle pressure ratio for nozzles having various expansion ratios and divergence angles.